# Evaluation of a Smartphone Sensor to Broadband and to Narrow Band Ultraviolet A Radiation

**Igoe, D.*,[1] and Parisi, A.V.[1]**

[1]Faculty of Health, Engineering and Sciences, University of Southern Queensland, Toowoomba, Australia

*Corresponding author: damienpaul@gmail.com

## Abstract

This research compares the smartphone image sensor response when exposed to broadband and narrow passband (340 nm and 380 nm) UVA wavelengths (320-400 nm) and builds on previous studies that have demonstrated that the smartphone image sensor is able to provide quantifiable response to narrow passband solar irradiances at 380 nm and 340 nm and can be used to reconstruct broadband UVA irradiances. This current research provides a comparison of the two main methods of ultraviolet irradiance observation and measurement, broadband and narrowband sensing, as applied to a common readily accessible smartphone. This research shows that the smartphone image sensor, with a broadband UVA filter possesses a strong sensitivity to long wavelength UVA irradiances from 370 nm, with a peak at 380 nm. However, the use of narrow passband and neutral density filters allows for quantifiable observations at the photobiologically important wavelength of 340 nm. Narrow passband filter observations also have far less variation at 340 nm than that observed for broadband measurements. The results indicate that the smartphone image sensor, with the addition of narrow passband and neutral density filters can be a viable tool for UVA observations, but is unsuitable for broadband measurements with a broadband filter.

## Introduction

The majority of ultraviolet reaching the Earth's surface, at 94% of total incoming UV radiation, is in the UVA waveband (320-400 nm)$^{(1)}$. The UVA waveband is further subdivided into UVA I (340 – 400 nm) and UVA II (320 – 340 nm) at approximately 340 nm, as the shorter wavelength UVA II has been found to cause DNA damage and a similar risk of skin cancer as UVB$^{(1,2)}$. The intensity of UV wavebands, are heavily dependent on aerosol load, solar zenith angle, surface albedo, seasonality, time of the day and observation elevation$^{(1,3-5)}$. The shorter UVA II wavelengths have more relative amounts of Rayleigh scattering than the UVA I. Additionally, UV spectral irradiances are particularly affected by shade and reflection from surrounding structures$^{(4,6)}$.

Traditional UVA irradiance measurement techniques either employ broadband measuring techniques, such as radiometers, or narrowband measuring techniques, such as employed in sunphotometers, spectroradiometers, Brewer spectrophotometers and narrow band filter instruments$^{(1,3)}$. Radiometers measure either the unweighted UV over a certain waveband or have a response that approximates a particular action spectrum$^{(7)}$. The Multifilter Rotating Shadowband Radiometer used by the United States Department of Agriculture, described by Bigelow et al.$^{(8)}$ uses seven nominal centre wavelengths that each need to be calibrated.

Smartphone image sensors with narrow pass band filters have been reported for the measurement of aerosol optical depth at 340 and 380 nm$^{(9,10)}$. These sensors use silicon photodiodes as complementary metal oxide semiconductor (CMOS) image sensors, which are sensitive, in situ, to incident UVA radiation$^{(9-12)}$. Experimentally, the CMOS image sensor has been found to respond to the magnitude of incident irradiance, rather than possessing any quantifiable dependence on wavelength(9,10). Thus, the use of a smartphone in measuring UVA irradiances would provide an inexpensive and accessible means to explore atmospheric pollution observations. Recent research by Igoe and Parisi(13) has demonstrated that solar broadband UVA irradiances can be reconstructed from the same discrete narrowband observations.

The focus of this research is to compare the smartphone image sensor response in the UVA waveband using broadband and narrowband filters, demonstrating that despite the inherent limitations, the CMOS smartphone image sensor can be used as a narrowband UVA irradiance device for scientific applications providing quantifiable responses to incident radiation at specific wavelengths. Thus, the smartphone image sensor can be used as a low-cost, accessible tool with narrowband filters to measure narrowband UVA irradiances, hence be used to reconstruct broadband UVA irradiances(13).

## Eperimental Method

Analysis was performed on sample broadband and narrowband UVA images taken using an off-the-shelf LG L3 smartphone (LG Electronics, Seoul, South Korea).

### *Broadband*

In order to investigate the response of the image sensor to broadband UVA, a broadband filter with diffuser (SED033/UVA/W, International Light, USA) with a UVA passband was affixed with a light tight seal over the sensor. This UVA broadband filter with diffuser will be referred to as the UVA filter in the remainder of the paper. The setup was evaluated in the field to take an image of the sun at a solar zenith angle of 14.6 degrees. This was repeated with a neutral density filter (ND2, supplier Bentham Instruments, UK) over the UVA filter to determine the response if saturation were to occur in the original image.

The spectral response of the UVA filter and smartphone image sensor was evaluated by characterising the response to narrowband irradiances from 320 nm to 400 nm at 10 nm intervals. The narrow band irradiances were provided with an irradiation monochromator with a xenon arc lamp (model 66390 Oriel Instruments, CA, USA) and monochromator with double gratings (model 74125 Oriel Instruments, CA, USA) in a laboratory with a temperature in the range 17°C to 24°C degrees. The full width at half maximum at each wavelength was 10 nm. The smartphone image sensor and UVA filter were setup, in a darkened room at a distance of 15 cm from the monochromator's exit slit, with the sensor plane normal to the beam, with the beam covering all of the sensor. For each wavelength three images of the beam were recorded with the phone camera settings left at their standard values. The irradiances for each wavelength setting were measured with a calibrated double grating monochromator spectroradiometer (model DMc150 Bentham Instruments Ltd. Reading, UK). The smartphone images, recorded in jpeg format containing eight bit red, green and blue data were processed using a specialised Android app, written and installed on the smartphone to determine the average digital number over the image of approximately 30 x 30 pixels of the solar disk(14); these results were verified by image analysis software. The process of image analysis involved the conversion of the red, green and blue image data for each pixel to a pixel digital number corresponding to the grayscale for each pixel(14).

The digital response variation was determined by taking a standard deviation of the pixel digital numbers for each image taken by the smartphone image sensor, providing an estimate of the noise present in each picture(15). This measure is important as it is also a gauge of pixel response stability when exposed to a specific wavelength.

### *Narrowband*

The response of the smartphone sensor to narrowband radiation using a narrowband array consisting of a 340 nm narrowband filter (CVI Melles Griot) and a 1% transmission neutral density (ND1%) filter (XND0001, Asahi Spectra) and a 380 nm narrowband filter (CVI Melles Griot) and a ND2 neutral density filter was reported using a laboratory source of an irradiation monochromator in Igoe et al.(9), for solar observations in Igoe et al.(10,13) and confirmed when tested as a smartphone app in Igoe et al.(14). Direct solar irradiances were observed by placing the narrowband filter array at the end of a black tube attached to the smartphone outer covering, to prevent light leakage into the image sensor, each photo was lined up with the sun using a zero-shadow method and three photos were taken. The image sensor responses were calibrated using a calibrated Microtops sunphotometer (Model E540, Solar Light) measuring the direct solar irradiances at 340 nm and 380 nm. The full width at half maximum of the Microtops is 2 nm. Direct irradiance observations were performed in solar zenith angle of between 60° and 5°.

## Results and Discussion

A comparison of the spectral transmissions of the UVA broadband and 340 nm and 380 nm narrowband filter arrays are shown in Figure 1. There is a clear strong transmission peak at approximately 360 nm in the broadband filter, whereas the narrowband filter arrays have substantially lower transmissions.

There is clearly saturation of the solar disk when the pictures were taken with the broadband filter, as was confirmed by image analysis. This saturation does not occur using the narrowband filter array used in Igoe et al.(10,14). The addition of the ND2 filter to the UVA filter results in no saturation, but results in the solar disk becoming indistinguishable.

Smartphone image sensors are not equipped to differentiate values from different wavelengths through a broadband filter. Specific wavelengths were provided with the irradiation monochromator as the wavelength of light could be pre-selected, but the wavelength differences cannot be detected by any algorithm or mechanism within the smartphone image sensor. To overcome this limitation, characterisation of the smartphone image sensor's response to UVA wavelengths was performed using the irradiation monochromator.

The characterised spectral response of the UVA filter and image sensor (Figure 2) indicates that the strongest response for both narrowband and broadband observations occurs at 380 nm where an additional ND2 filter was still required to prevent saturation at this wavelength. For each wavelength, three images were taken of 30 x 30 pixels and the plotted data points are the average of these 2,700 data points. The standard deviation of these 2,700 data points is an error bar that is within the symbol of the plotted data. The Figure shows that the 380 nm wavelength dominates the broadband spectral response, with any wavelengths shorter than 370 nm providing digital number values less than background noise levels, compared with a stronger narrowband response at 340 nm.

Previous laboratory and field studies(9,10,14) have shown that the smartphone camera, with calibration to the irradiances from the calibrated Microtops photometer, can quantify the level of narrowband irradiance (from any UV source) using narrowband filter arrays with narrowband filters at 340 nm and 380 nm, with the latter requiring the additional ND2 filter to prevent saturation. The waveband from the irradiation monochromator possesses a full width at half maximum of 10 nm, whereas the Microtops is 2 nm. However, as the narrowband filter arrays were found to have a comparable full width at half maximum as that of the irradiation monochromator, thus a comparison can be made between the two sources.

In comparison, narrowband solar UVA observations for 340 nm and 380 nm filter arrays have lower variation for 340 nm and comparable relative variation at 380 nm than the broadband filter monochromator characterisation (Figure 3).

The increase in broadband image sensor response (Figure 2) corresponding to the sharp decrease in variation (Figure 3) at 370 nm is likely due to the limitations of the silicon-based photodiodes that make up the CMOS image sensor. However, this pattern is less prominent with narrowband observations. Though the actual parameters of the silicon photodiodes are proprietary information, the reason can be inferred from the analysis by Green and Keevers(11) of the optical properties of silicon, where there is an exponential increase in absorption from 370 nm.

## Conclusion

A smartphone image sensor with a UVA filter is responsive to broadband UVA wavelengths of 370 to 400 nm, but not the shorter UVA wavelengths. The response to this array is not flat across the UVA waveband to allow measurement from 320 to 400 nm. In comparison, the use of narrow pass band filters with neutral density filters at discrete wavelengths enables the measurement of irradiances at UVA wavelengths less than 370 nm, allowing for narrowband measurements to be used to reconstruct broadband irradiances.

References

1. Diffey, B. What is Light? Photodermatol. Photoimmunol. Photomed. 2002, 18, 68-74.
2. Edstrom, D.; Porwit, A.; Ros, A. Effects on Human Skin of Repetitive Ultraviolet-A1 (UVA1) Irradiation and Visible Light. Photodermatol. Photoimmunol. Photomed. 2001, 17, 66-70.
3. Meloni, D.; Marenco, F.; di Sarra, A. Ultraviolet Radiation and Aerosol Monitoring at Lampedusa, Italy, Annals of Geophys, 2003, 46, 373-383.
4. Parisi, A.V.; Sabburg, J.; Kimlin, M. Scattered and Filter Solar UV Measurements; Dordrecht, Kluwer Academic Publishers, 2004; 195p.
5. Piervitali, E.; Benedetti, E.; Damiani, A.; Rafanelli, C.; Di Menno, I.; Casu, G.; Malaspina, F.; Anav, A.; Di Menno, M. Evaluation of Environmental UV Doses by Empirical WL4UV Model and Multichannel Radiometer. In Ultraviolet Ground- and Space-Based Measurements, Models, and Effects V, Proceedings of SPIE, vol. 5886, Bellingham, WA, USA; Bernhard, G., Slusser, J., Herman, J., Gao, W. Eds.; 2005.
6. Turner, J.; Parisi, A.V. Influence of Reflected UV Irradiance on Occupational Exposure from Combinations of Reflective Wall Surfaces, Photochem. Photobiol. Sci. 2013, 12, 1589-1595.
7. Anav, A.; Rafanelli, C.; Di Menno, I.; Di Menno, M. An Algorithm to Evaluate Solar Irradiance and Effective Dose Rates using Spectral UV Irradiance at Four Selected Wavelengths. Rad. Prot. Dos. 2004, 111, 239-250.
8. Bigelow, D.; Slusser, J.; Beaubien, A.; Gibson, J. The USDA Ultraviolet Radiation Monitoring Program. Bull. Am. Met. Soc. 1998, 79, 601-615.
9. Igoe, D.; Parisi, A.V.; Carter, B. Characterisation of a Smartphone Response to Ultraviolet A Radiation. Photochem. Photobiol. 2013, 89, 215-218.

10. Igoe, D.; Parisi, A.V.; Carter, B. Evaluating UVA Aerosol Optical Depth using a Smartphone. Photochem. Photobiol. 2013, 89, 1244-1248.
11. Green, M.; Keevers, M. Optical Properties of Intrinsic Silicon at 300K. Progress in Photovoltaics. 1995, 3, 189-192.
12. Haapalinna, A.; Karha, P.; Ikonen, E. Spectral Reflectance of Silicon Photodiodes. *Appl. Optics*, 1998, 37, 729-732.
13. Igoe, D. Parisi, A.V. Broadband Direc UVA Irradiance Measurement for Clear Skies Evaluated using a Smartphone. Rad. Prot. Dos. 2014, doi:10.1093/rpd/ncu344
14. Igoe, D.; Parisi, A.; Carter, B. Smartphone-Based Android App for Determining UVA Aerosol Optical Depth and Direct Irradiances. Photochem. Photobiol. 2014, 90, 233-237.
15. Irie, K.; McKinnon, A.; Unsworth, K.; Woodhead, I. Measurement of Digital Camera Image Noise for Imaging Applications. Sensors and Transducers, 2008, 90, 185-194.

**Figure Captions**

Figure 1: Comparison of spectral transmissions of the UVA broadband filter compared to the narrowband filter arrays. The diamonds represent observations from the UVA broadband filter and the squares are discrete measurements from the narrowband filter array. The line represents the reconstructed UVA broadband transmission.

Figure 2: Smartphone image sensor spectral response with the UVA broadband filter, positioned 15 cm from the exit slit of an irradiation monochromator. The diamonds represent observations from the UVA broadband filter, the squares are discrete measurements from the narrowband filter array. The line represents the reconstructed UVA broadband response from the image sensor. Unless visible, error bars (standard deviation) are too small to be seen.

Figure 3: Relative variation of narrowband UVA observations compared to broadband UVA monochromator characterisation observations.  The diamonds represent observations from the UVA broadband filter and the squares are discrete measurements from the narrowband filter array.

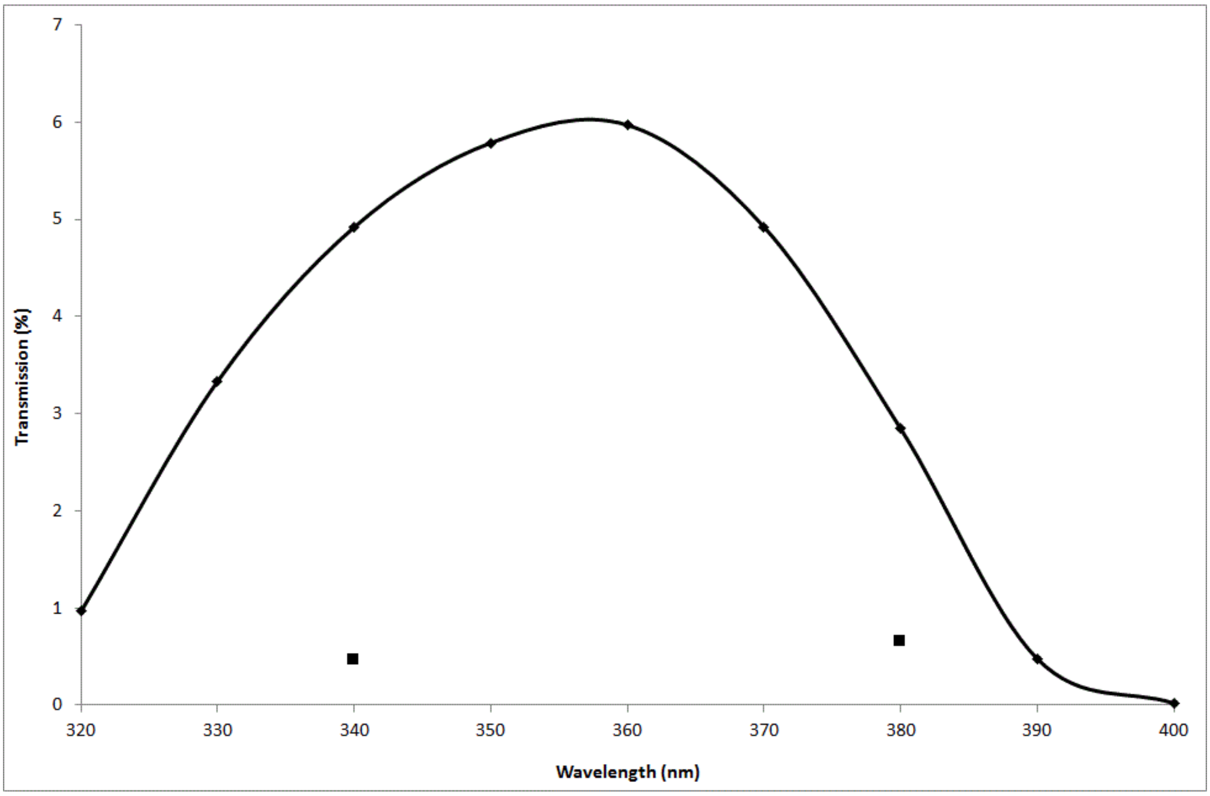
Transmission (%)
0
1
2
3
4
5
6
7
320
330
340
350
360
370
380
390
400
Wavelength (nm)

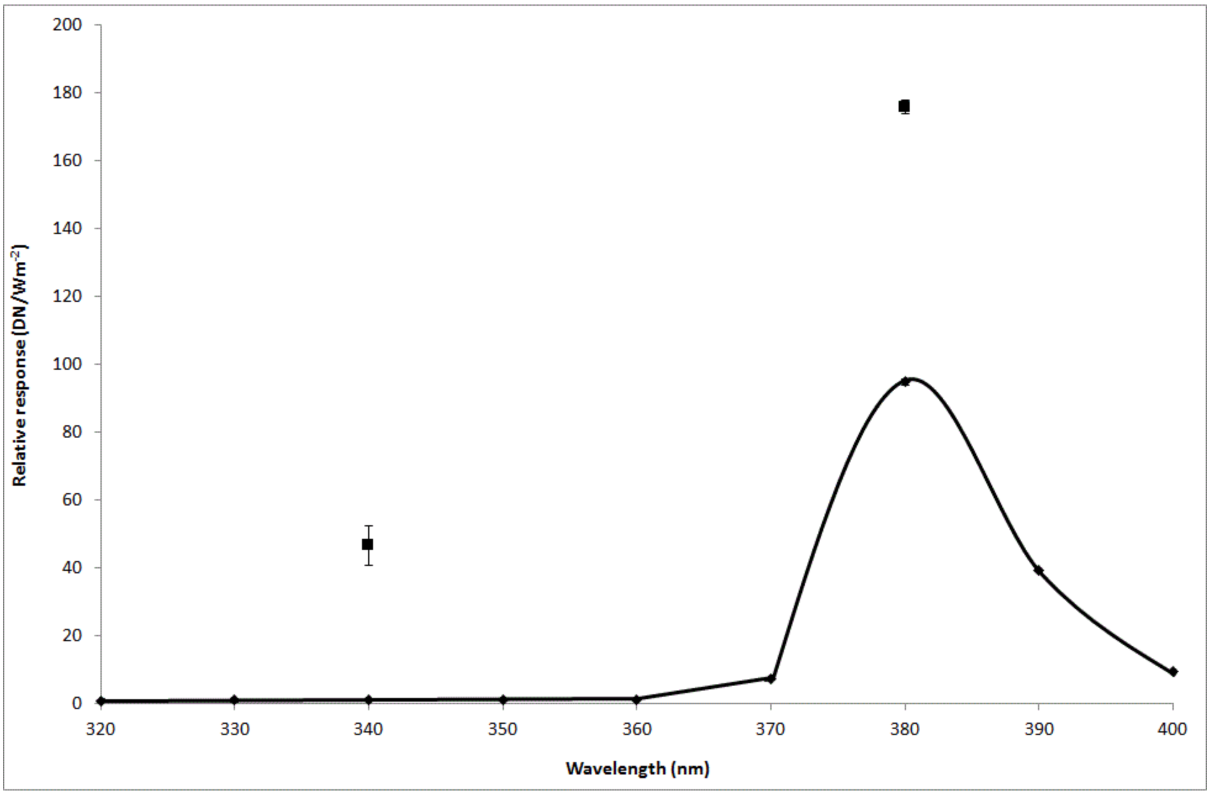
200
180
160
140
120
100
80
60
40
20
0
Relative response (DN/W/m$^{-2}$)
320
330
340
350
360
370
380
390
400
Wavelength (nm)

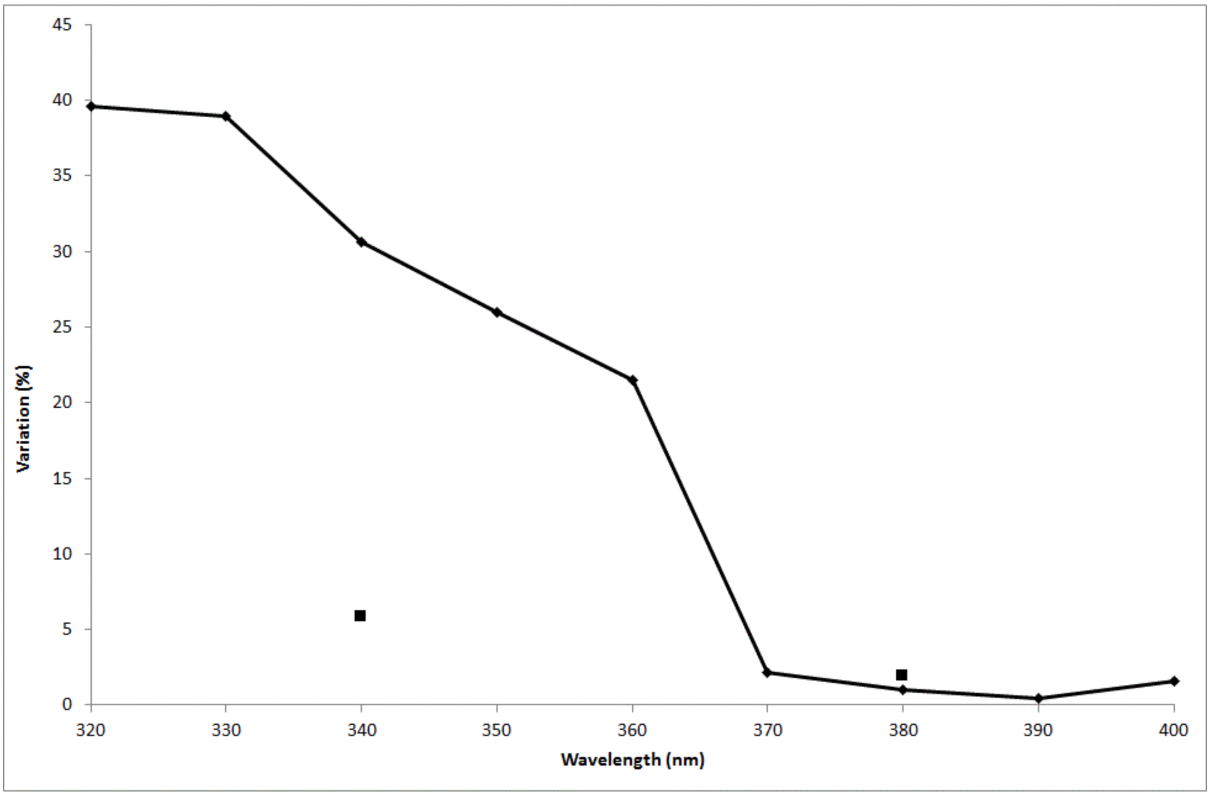
Variation (%)
45
40
35
30
25
20
15
10
5
0
320
330
340
350
360
370
380
390
400
Wavelength (nm)